Approach for numerically describing and classifying benthic animals' polymorphic cells morphology

Yuri A. Karetin[1,2], Eduardas Cicinskas[1]

[1]Far Eastern Federal University, FEFU Campus, Vladivostok, Russia

[2]A.V. Zhirmunsky Institute of Marine Biology FEB RAS, Palchevskogo, Vladivostok, Russia

Corresponding Author:

Eduardas Cicinskas

FEFU Campus, Vladivostok, 690922, Russia

Email address: cicinskas@gmail.com

Abstract

Describing cell morphology is a tricky task, prone to misinterpretation due to subjective nature of the human observer and his vocabulary limitations. Consequently, these limitations actuate prevalence of non-formalized, statistically unverifiable language use. This determines the reason for overlooking cell shape as a viable parameter for describing cell's functional state intricacies. In this study we demonstrate the use of mathematical parameters set for describing two-dimensional fractals, such as: convex hull, density, roundness and asymmetry, for comparative in vitro morphological analysis of sprawled starfishes' Aphelasterias japonica and Patiria pectinifera (Echinodermata: Asteroidea) coelomocytes, and bivalve's Callista brevisiphonata (Mollusca: Bivalvia) hemocytes. We found that these parameters allow us to describe visually distinguishable but verbally indescribable "chaotic" sprawled cell shapes. Furthermore, resulting numerical cell descriptions differs significantly, enabling for their species-specific grouping and classification. We argue that presented morphometric methodology can be used for describing and classifying cells of any arbitrary morphology, as well as compiling "cell shape - cell functional state" match library for later use in *in vitro* analysis, potentially for cells of any animal.

Key Words: Callista brevisiphonata; Aphelasterias japonica; morphometry; Patiria pectinifera; hemocyte; coelomocyte; benthic animals; immune system

Introduction

The traditional classification of marine invertebrates' hemocytes and coelomocytes consists of a variety of cytological (e.g., cytoplasm granularity, nuclear-cytoplasmic ratio, nuclear chromatin structure), biochemical (e.g., presence of various enzymes), and functional (e.g., phagocytotic ability, granule exocytosis, adhesion to a substrate) characteristics (Duarte 2012; Hine 1999; Martin 1990). However, these parameters are not static, as majority of invertebrates' hemolymph's and coelomic fluid's cells are poorly specialized - transformations from one cell type to another have been observed in some species (Yamashita 2001; Dyrynda 1997; Fisher 1986). Enzymatic content, cytoplasmic granularity, and other morphological and

functional characteristics vary greatly depending on the functional state of the animal organism (Anisimova 2013; Danielli 2011; Martin 1992). Never the less, these parameters are still used for describing and classifying these cells, whilst approaches for differentiating cells based on their sprawling characteristics are undeservedly overlooked. Previously we conducted an visual analysis of cell sprawling in at least ten marine invertebrate species, which clearly demonstrated species-specific sprawling traits (unpublished data). These differences in flattened cell morphology should carry as much biological context as any other more conventional morphometric parameter, because sprawling cell's shape is determined by interactions of complicated matrix-receptor-cytoskeleton complexes (Yuhang 2013), various genetic and epigenetic variations in cell's functional state (Kolyuchkina 2011), degree of substrate adhesion (Rioult 2013), expression of cell surface receptor sets (Jiun-Hong 1995), and composition or dynamics of cytoskeletal structure (Chernyavskikh 2012). These variables are close among cells of same-species animals and should respond similarity to the same external and internal stimuli, influencing cell's sprawling morphology. Therefore, interpretation of statistically significant numerical parameters describing changes in cell's morphology may be used to determine the presence of various natural and/or artificial factors affecting cell's functional state.

Materials and Methods

Animal cells

628 bivalve's Callista brevisiphonata (Bivalvia, Veneridae) (Carpenter 1864) hemocytes, 569 starfish Aphelasterias japonica (Echinodermata: Asteroidea)(Bell 1881) coelomocytes, and 410 starfish Patiria pectinifera (Echinodermata: Asteroidea)(Muller & Troschel 1842) coelomocytes were examined in this study. Animals were harvested in 10-15th of September in the Vostok Bay (waters of the Peter the Great Gulf, Primorsky Krai). Immediately following collection, animals were necropsied. Syringe was used to collect hemolymph from mollusc's pericardial and mantle cavities, and starfishes' coelomic cavity. Immediately after collection, cells were placed onto cover glass, where they were held at room temperature for an hour and fixed with 4% formalin seawater solution. Fixed cells were stained with hematoxylin and eosin, dehydrated, and embedded into Canada balsam.

74

75 Cell visualization

76

77 Zeiss Axiovert 200M Apotome microscope was used for visualization. Two-dimensional
78 contours of sprawled cells were sketched by hand from the tabled computer screen onto
79 transparencies, which were later scanned for further processing. A single pixel outline of the
80 external cell boundary was used to generate cell's contour image. Contour images were later
81 filled to generate cell silhouettes.

82

83 Image processing

84

85 Pictures of cells were digitized and converted into a one-bit format. A fractal analysis was
86 performed using a FracLac 2.5 plugin for ImageJ 1.41 image analysis software. The linear
87 parameters were counted using ImageJ 1.41 and Photoshop SC3.

88 14 cell shape descriptors were used: *Area*; *Circularity*: 4π*area / perimeter^2, (***Circ***);
89 *Feret's Diameter* – the longest distance between any two points along the object boundary, also
90 known as maximum caliper, (***Feret***); *Aspect ratio*: major_axis/minor_axis of object, (***AR***);
91 *Roundness*: 4*area /(π*major_axis^2), (***Round***); *Density*=Foreground Pixels/Hull Area, (***Density***);
92 *Hull's Perimeter* – perimeter of the convex hull drawn around the object, (***Hull'sPer***); *Hull's*
93 *Circularity* – Circularity of the convex hull = 4π*area / perimeter^2, (***Hull'sCirc***); *Max/Min Radii*
94 *from Hull's Centre of Mass* – the ratio of maximum and minimum radii from the centre of
95 mass for the convex hull to an exterior point, (***M/MHull'sCM***); *Max/Min Radii from Circle's*
96 *Centre* – The ratio between the maximum and the minimum radii from the circle's centre to a
97 point on the convex hull, (***M/M RadCirc***); *Perimeter* of cell, (***Per***); *Roundness* of the outline
98 picture of cells, (***Round out***). For more details about the nonlinear parameters, see the software
99 website: http://rsbweb.nih.gov/ij/plugins/fraclac/FLHelp/UseFracLac.htm.

100 We also used our own parameters, describing cell asymmetry: ratio of two circular
101 segment areas, which were generated by drawing a line over an encircled cell image dividing it
102 into two most uneven parts **(1/2half)**; ratio of encircled cell's cell-free and cell's areas
103 **(in50/out50)**.

104

Statistical analysis

Statistical analysis was carried out using STATISTICA 6.0 and NCSS 2007. Paired differences between characteristics were tested using the independent samples t-Test. Correlation between parameters was measured with Pearson's linear correlation analysis. Results were considered significant when $P<0.05$.

Highly correlated parameters, such as those describing the similar morphological properties and having similar mutual arrangement of the mean values and standard error of the mean, among cells of all studied species, were excluded from the analysis. The factor analysis reduces the model dimensionality by describing the variance represented by the original parameters in terms of a smaller number of latent variables (Uberla 1997; Gordon 1999). We used R-mode factor analysis. The factors were extracted by using principal axis factoring and orthogonally rotated by using varimax rotation. The number of significant factors was chosen using Kaiser criterion, Cattell scree plot test and interpretability of factors (Uberla 1997; Costello and Osborne 2005).

Results and Discussion

Invertebrate hemolymph and coelomic fluid's cells serve a protective function, implementing specific cellular responses upon encountering a foreign body: phagocytosis – devourment of detected microscopic particles, encapsulation - cell flattening along the foreign body too large to be phagocytosed, and, if foreign body's surface greatly exceeds cell's size - sprawling over the substrate in an attempt to isolate it (Ratner 1983).

Within few minutes of placing hemolymph onto artificial substrate its cells settle, adhere, form different size conglomerates and flatten, forming either almost continuous cell coating, or a network of contiguous pseudopodia of self-assembled into cell-streams cells. Predominance of conglomeration over flattening is species-specific and depends on whether adhesion to substrate prevails over intercellular adhesion (Isayev 1994). This ratio may also vary depending on the cultivation conditions. For example, bivalve's *Mizuhopecten yessoensis* hemocytes predominantly form aggregates when cultivated with the addition of autologous hemolymph or

FBS, and leave the aggregates to flatten over a substrate, if seawater is used instead (Demenok 1997).

Examined marine invertebrate's cells formed a wide range of various shapes: from round cells with poorly developed boundaries, to cells with complex irregular shapes with long pseudopodia and fractal outlines as a result of maximum flattening. Cells of all studied animals were clearly visually distinguishable, but the differences could hardly be conveyed using verbal terms. This extreme variability of shapes determines hemocytes and coelomocytes as an ideal model for testing suggested morphometric methodology.

Contrary to neuron morphology which's classical morphometry is well developed (Pushchin 2014), morphological description of flattened fibroblast-like cells *in vitro* is hardly formalized. Meanwhile, an overwhelming number of studies exploring the influence of biochemical, morphological, physiological, and genetic parameters in cell behavior changes during cell shape transformation use statistically unverifiable language for describing cell shape. Usually, *in vitro* morphometric studies of sprawling cells concentrate on a rather narrowly-specific problems and use methodology which can be used for describing shapes of only certain cell types, cultured under highly specific conditions (Kozlowski 2012; Xiong 2010). This narrowing is a result of a wide chaotic variety and "abnormality" of shapes of various species' flattened cells. Usually, attempts to describe a whole range of possible amoeboid cells shapes *in vitro* result in a set of rather generalized, non-specific morphometric parameters, describing only general features of a two-dimensional objects, such as: object's area, convex hull's area, roundness, or density. However, if suggested methodology which provides a numerical description of cell's morphology is demonstrated to work with a wide variety of cell shapes, it could effectively replace the non-formalized language used to describe and classify cell morphology in most of studies.

Methodology suggested in this research uses parameters describing cell's roundness, convex hull properties, circumcircle, asymmetry relative to the optical center, and density. Therefore, the full spectrum of characteristics applicable to a non-specific two-dimensional one-bit images of "abnormal", from the viewpoint of Euclidean geometry, shapes, any of which could be taken by studied cells, was covered.

A factor analysis grouped all parameters into 3 factors consisting of characteristics describing different aspects of cell's morphology. Factor 1 included cell size characteristics, such

as: Area and Hull'sPer; factor 2 was loaded with parameters describing roundness and cell elongation: Round, Hull'sCirc, MMHull'sCM, and MMRadCirc; factor 3 reflected various features of cell asymmetry: in50/out50 or 1/2half. The factor load was species-specific in some cases, but generally, the same loadout was used for cells of all species. As a result, all investigated characteristics were grouped into three categories with a detectable level of correlations amongst parameters inside single category. These were categories describing cell's dimensional characteristics, roundness, and asymmetry.

Some characteristics demonstrated high correlation levels in all studied cells, while others were species-specific (Table 1). For example: cell area and convex hull - parameters describing the overall cell size were highly correlated in cells of all three species (r=0.90, 0.72, and 0.85 in *A. japonica*, *C. brevisiphonata*, and *P. pectinifera*, respectively). Lowest correlation with *C. brevisiphonata* cells can be explained by the fact that their cells have longest and thinnest pseudopodia. Relatively small cell body combined with extremely long (several times exceeding cell body diameter) pseudopodium, significantly increases convex hull perimeter, whilst insignificantly increasing total cell area.

Another example: species-specific correlations of Circ and Hull'sPer, which were almost not correlated in coelomocytes of A. japonica, weakly anti-correlated in hemocytes of C. brevisiphonata, and strongly anti-correlated in coelomocytes of P. pectinifera (r=-0.36; -0.58; -0.80, respectively). This difference in correlation suggest that these parameters describe slightly different cell morphological aspects in different species, correlation between which is not so obvious. Circ was lowest in large P. pectinifera cells, which were highly fragmented - their cytoplasm densely stacked with droplets. P. pectinifera Circ values were magnitudes lower than minimal Circ of A. japonica cells which had virtually no fragmentation. The smallest Circ in this species belonged to a heterogeneous group of rod-like cell sub-population, with partially fragmented cytoplasm and well developed microsculpture, presented as pseudopodia of varying sizes. In P. pectinifera highest values of Hull's Perimeter corresponded to cells with highly fragmented cytoplasm. This determined anti-correlation of Circ and Hull's Perimeter, however cell morphology was highly varying: among P. pectinifera cells with highest Hull's Perimeter values, there were cells with highly fragmented droplet-shaped cytoplasm, cells with various kinds of convexities, and, something exclusive for P. pectinifera – rounded nubs at the pseudopodia ends. This explains significant differences in correlation between these parameters

among cells of this species. The maximum values of Hull's Perimeter in *A. japonica* cells corresponded to cells with a varying Circ parameter values: among these cells there were none with simple microsculpture, however this level of fractal boundaries was found among cells with average Hull's Perimeter, making visual identification of a morphological property determining high of Hull's Perimeter values impossible (Fig. 1 a-b).

Another pair: Round and Hull'sCirc, were maximally correlated in *A. japonica cells* and least correlated in *C. brevisiphonata* (0.80 and 0.47, respectively). The minimum values of Round in cells of both species correspond to elongated rod-shaped cells. The maximum values of Round in *A. japonica* corresponded to rounded cells without long asymmetric pseudopodia. On the other hand, in *C. brevisiphonata* high Round values coincided with both rounded cells and cells of an irregular shape, with one or more long, asymmetrically arranged, pseudopodia. Round is calculated as a ratio of cells area to cell main axis length, i.e. degree of elongation or roundness of the ellipse encircling the cell. This allows for a high degree of freedom in cell shape. In both species, smallest Hull'sCirc values correspond to elongated cells, whilst highest Round values are typical for cell with a more rounded shape. This makes Hull'sCirc ideal for describing cell roundness, and Round – its elongation. Unlike *C. brevisiphonata*, *A. japonica* coelomocytes rarely had a single, long processe, nor was their cytoplasm fragmented as in *P. pectinifera* coelomocytes. This fitted their cells into “elongated - rounded” dualism framework, which is simultaneously described by both Round and Hull'sCirc, whereas hemocytes of *C. brevisiphonata* are take-up a much larger variety of asymmetric shapes with long processes, which determines the lack of correlation between these parameters in this species (Fig. 1 b-c).

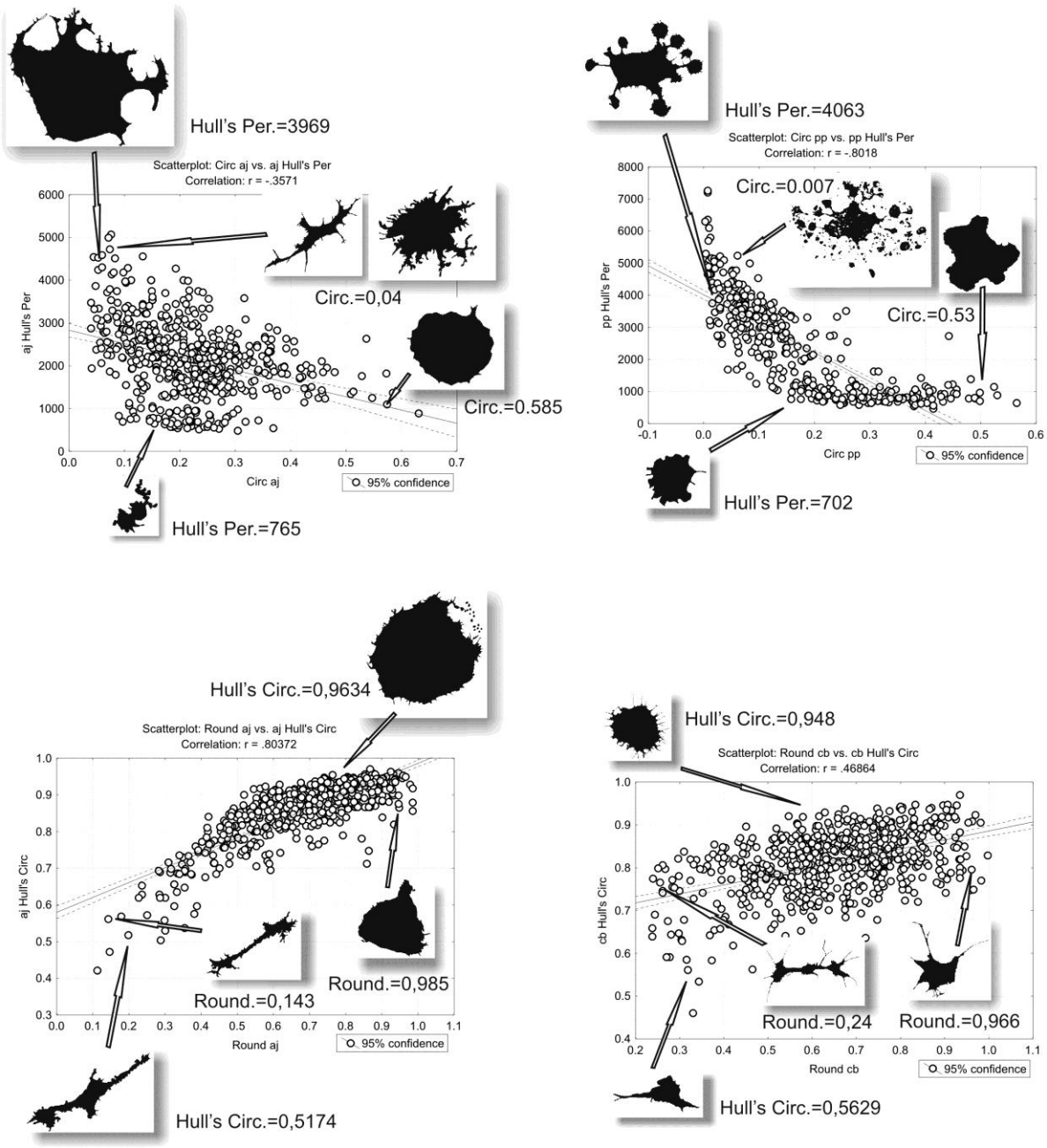

Fig. 1 Scatterplots of (a.) Circularity vs Hull's Perimeter, A. Japonica; (b.) Circularity vs Hull's Perimeter, P. pectinifera; (c.) Roundness vs Hull's Circularity, A. Japonica; (d.) Roundness vs Hull's Circularity, C. Brevisiphonata

Out of 14 parameters selected for the analysis, 3 parameters, which were highly correlated (r>=0.9) with all of the other parameters and similar mutual ratio of mean values among cells of all three-studied species, were excluded. Among remaining parameters, mean

227 standard error of some were overlapping, and those that remained could reliably separate cells
228 among two, and, more rarely – of all three species. *A. japonica* cells could be characterized by
229 significantly high Round, Circ, Hull'sCirc, and MMHull'sCM, and low Hull'sPer values. *C*
230 *brevisiphonata* cells could be identified by highest Hull'sPer, 1/2half, and in50/out50 and lowest
231 Circ and Density. *P. pectinifera* cells had smallest Area values, and average, but statistically
232 distinguishable from the rest Circ and Hull'sPer values (Fig. 2).
233

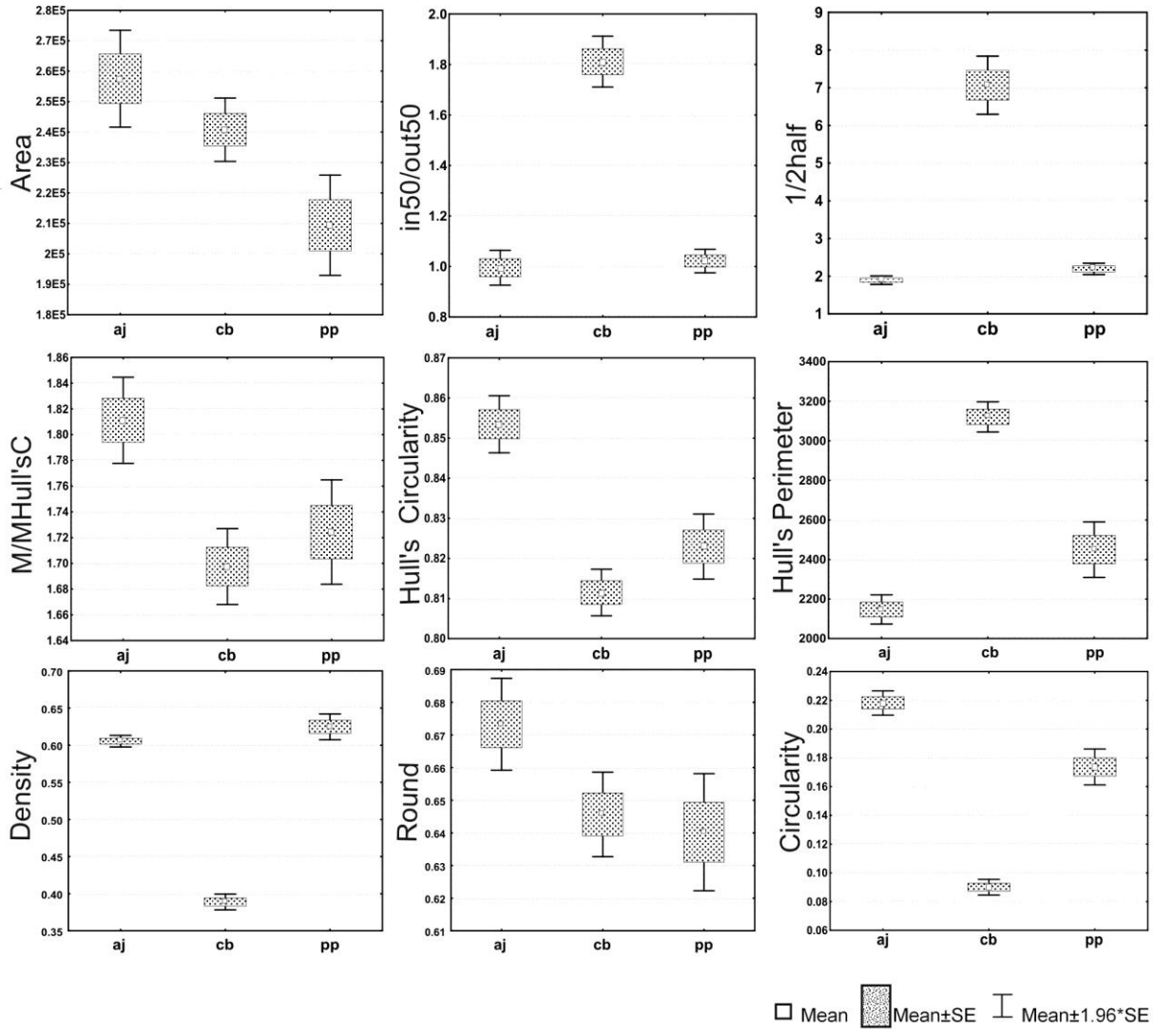

234
235 Fig. 2 Mean values of parameters that reliably distinguish cells from at least one of the
236 species from cell of two other species. aj - Aphelasterias japonica, cb - Callista brevisiphonata,
237 pp - Patiria pectinifera

Chosen parameters formed "cell's digital profile" - a set of numeric values which reliably distinguished cells from all three studied invertebrate species among themselves. This digital profile was specific to cells of same species and distinguishes them from cells of other species (see Table 2). Paired comparison using t-test always resulted in statistically significant differences between cells of any two species (see Table 3).

When exploring cell morphology, the main interest, from the biological viewpoint, is identification of factors determining flattened hemocytes and coelomocytes morphology in different invertebrates species. Initial hypothesis suggested searching for ecological aspects for cell functional differences, which are reflected in the cell's morphology and dictate cells shape variations among studied animals. However, we did not find any significant environmental differences. *C. brevisiphonata* lives on sandy and sandy-aleuritic sediments at depths ranging from 8-10 to 30-40 m, burrowing at shell-depth into the bottom layer. *P. pectinifera* inhabits sandy, rocky, and silty grounds up to a depth of 40 m. *A. japonica* inhabits rocky grounds up to depths of 40-50 m, more rarely - on silty sands with an admixture of pebbles and rocks, shell deposits. *C. brevisiphonata* is suffering from predation by starfishes of both species. All animals were collected from the same area and constitute the most common species of invertebrates in that area. Previously we suggested that intercellular adhesion with subsequent cell aggregates retraction *in vitro* predominates in bivalve hemocytes, because it mimics *in vivo* thrombosis and wound contraction after sustaining an injury. In echinoderms, this retraction is absent due to rigidity of the external integuments, and adhesion to a substrate predominates (Demenok 1997). However, this assumption was correct only for *M. yessoensis*, which's hemocytes form large retracting conglomerates *in vitro* (Dziuba 1992). In cells of other bivalve species, including those explored in this study, as well as in echinoderm coelomocytes, adhesion to the substrate prevails over intercellular adhesion and retracting aggregates are not formed. But regardless of whether environmental differences determine hemocytes and coelomocytes shapes in different species and whether nuances of their morphology are subjected to the natural selection, it seems certain that cell shape is genetically determined as a result of certain cell physiology nuances, such as the cytoskeleton structure, cell behavior, etc. Therefore, identifying underling genetic and cytophysiological changes in species-specific cellular response and tying them with definite cell shapes seems logical. This enables for prediction of cell's physiological features under normal

and pathological conditions using only detailed morphological analysis. This approach also provides a methodological basis for environmental monitoring, since functional changes in cell immunity of widespread species are indicators of environment's ecological state, and, consequently, it's inhabitants health state (Canesi, 2007; Bouilly 2006; Isayev 1995).

Conclusion

The species-specific marine invertebrates' hemolymph and coelomic fluid's cell behavior can be statistically significantly described by a set of numerical values, characterizing sprawling cell's shape, such as: roundness, density, elongation, asymmetry, and its dimensional characteristics, like: size, circumcircle, and convex hull. Whether suggested methodology can differentiate between cells under various natural or artificial conditions, as well as its applicability to classify cells of phylogenetically related species, remains unanswered.

Here we demonstrated that suggested methodology can be used to numerically describe *in vitro* sprawled cell shapes of different marine invertebrates' species, generating cell's digital profile which could be used for statistically significant comparison. This method effectively complements classical methods for *in vitro* description of marine invertebrates' immune cells, but is not limited to them, and theoretically can be used for vertebrates' cells as well, due to generality of structural and functional properties in both taxa (Browne 2013).

References

Anisimova AA (2013) Morphofunctional parameters of hemocytes in the assessment of the physiological status of bivalve. *Russian Journal of Marine Biology* 39(6):381-391.

Bouilly K, Gagnaire B, Bonnard M, Thomas-Guyon H, Renault T, Miramand P, Lapègue S (2006) Effects of cadmium on aneuploidy and hemocyte parameters in the Pacific oyster Crassostrea gigas. *Aquatic Toxicology* 78: 149–156.

Browne N, Heelan M, Kavanagh K (2013) An analysis of the structural and functional similarities of insect hemocytes and mammalian phagocytes. *Virulence* 4(7):597-603. https://doi.org/10.4161/viru.25906.

Canesi L, Ciacci C, Betti M, Fabbri R, Canonico B, Fantinati A, Marcomini A, Pojana G (2008) Immunotoxicity of carbon black nanoparticles to blue mussel hemocytes. *Environment International* 34(8):1114–1119.

Cavalcanti MGS, Filho FC, Mendonca AMB, Duarte GR, Barbosa CCGS, De Castro CMMB, Alves LC, Brayner FA (2012) Morphological characterization of hemocytes from Biomphalaria glabrata and Biomphalaria straminea. *Micron* 43(2-3):285-291. https://doi.org/10.1016/j.micron.2011.09.002.

Chernyavskikh SD, Fedorova MZ, Thanh VV, Quyet DH (2012) Reorganization of actin cytoskeleton of nuclear erythrocytes and leukocytes in fish, frogs, and birds during migration. *Cell and Tissue Biology* 6(4):348-352.

Costello AB, Osborne LW (2005) Best practices in exploratory factor analysis: four recommendations for getting the most from your analysis. *Practical Assessment, Research & Evaluation* 10: 1–9.

Danielli GP, Carmem SF (2011) Hemocitical responses to environmental stress in invertebrates: a review. *Environmental Monitoring and Assessment* 177(1-4):437-447.

Demenok LG, Karetin YuA, Isaeva VV (1997) In vitro aggregation of hemocytes of the Japanese scallop Mizuhopecten yessoensis. *Russian Journal of Marine Biology* 23(5):327-329.

Dzjuba SM, Romanova LG (1992) Morphology of amoebocytes of the Japanese scallop hemal system. *Tsitologiya* 10(34):54-60.

Dyrynda EA, Pipe RK, Ratcliffe NA (1997) Sub – populations of haemocytes in the adult and developing marine mussel, Mytilus edulis, identified by use of monoclonal antibodies. *Cell & Tissue Research* 289:527-536.

Gordon AD (1999) Classification. New York: Chapman & Hall/ CRC.

Fisher WS (1986) Structure and functions of oyster hemocytes. In: Brehelin M, Arcier JM, Boemare N, Bonami JR, Vivares CP (ed) Immunity in Invertebrates, Springer-Verlag Berlin Heidelberg, pp 25-35.

Hine PM (1999) The interrelationship of bivalve haemocytes. *Fish & Shellfish Immunology* 9:367-385.

Isaeva VV (1994) Cells in morphogenesis. Nauka, Moscow.

Isaeva VV (1995) The use of mollusc hemocytes and echinoderm coelomocytes for bioassay. *Russian Journal of Marine Biology* 21(6):378-385.

Chen J-H, Christopher JB (1995) Hemocyte adhesion in the California mussel (Mytilus californianus): regulation by adenosine. *Biochimica et Biophysica Acta (BBA) - Molecular Cell Research* 1268(2):178–184.

Kolyuchkina GA, Ismailov AD (2011) Morpho-functional characteristics of bivalve mollusks under the experimental environmental pollution by heavy metals. *Oceanology* 51(5):804-813.

Kozlowski C, Weimer RM (2012) An Automated Method to Quantify Microglia Morphology and Application to Monitor Activation State Longitudinally In Vivo. *PLoS ONE* 7(2):e31814. https://doi.org/10.1371/journal.pone.0031814.

Martin GG, Hose JE, Gerard AS (1990) A decapode classification scheme integrating morphology, cytochemistry and function. *The Biological Bulletin* 178:33-45.

Martin GG, Hose JE (1992) Vascular elements and blood (Hemolymph). *Microscopic Anatomy of Invertebrates* 10:117-146.

Pushchin I, Karetin Y (2014) Retinal ganglion cells in the Pacific redfin, Tribolodon brandtii dybowski, 1872: morphology and diversity. *Journal of Comparative Neurology* 522(6):1355-72. https://doi.org/10.1002/cne.23489.

Rioult D, Lebel JM, Foll FL (2013) Cell tracking and velocimetric parameters analysis as an approach to assess activity of mussel (Mytilus edulis) hemocytes in vitro. *Cytotechnology* 65(5):749-758.

Ratner Sб Vinson SB (1983) Phagocytosis and Encapsulation: Cellular Immune Responses in Arthropoda. *American Zoologist* 23(1):185-194. https://doi.org/10.1093/icb/23.1.185.

Uberla K (1997) Faktorenanalyse. Berlin: Springer-Verlag.

Xiong Y, Iglesias PA (2010) Tools for analyzing cell shape changes during chemotaxis. *Integrative Biology (Camb)* 2(11-12):561-7. https://doi.org/10.1039/c0ib00036a.

Yamashita M, Iwabuchi K (2001) Bombyx mori prohemocyte division and differentiation in individual microcultures. *Journal of Insect Physiology* 47(4-5):325-331.

Yuhang H, Xiaozhen Y, Yongxu Ch, Pan L, Jinbiao Z, Meng Li, Cheng Sh., Zhigang Y, Chun W (2013) Effects of pH, temperature, and osmolarity on the morphology and survival rate of primary hemocyte cultures from the Mitten Crab, Eriocheir sinensis. *In Vitro Cellular & Developmental Biology – Animal* 49(9):716-727.

Tables

	Area												
Circ.	-0.20 -0.21 0.63	Circ.											
Feret	0.83* 0.65* 0.85*	-0.40† -0.58† -0.78†	Feret										
AR	-0.17 -0.11 0.10	-0.28 -0.11 -0.25	0.23 0.22 0.36	AR									
Round	0.25 0.16 -0.12	0.29 0.12 0.27	-0.14 -0.19 -0.37	-0.84* -0.93* -0.93*	Round								
Density	-0.44 0.08 -0.49	0.74* 0.83* 0.66*	-0.10 -0.55 -0.64	0.53 -0.19 -0.44	-0.56 0.21 0.44	Density							
Hull'sPer	0.90* 0.72* 0.85*	-0.36† -0.58† -0.80†	0.98* 0.98* 0.96*	0.08 0.12 0.23	0.03 -0.08 -0.24	-0.21 -0.53 -0.53	Hull'sPer						
Hull'sCirc	0.29 0.37 -0.11	0.28 0.10 0.43	-0.18 -0.11 -0.44	-0.82† -0.47† -0.76†	0.80† 0.47† 0.75†	-0.67 0.26 0.43	-0.003 0.03 -0.37	Hull'sCirc					
M/M Hull'sCM	-0.05 -0.19 -0.28	-0.01 0.10 0.35	0.15 0.03 -0.23	0.34 -0.47 0.35	-0.42 -0.34 -0.38	0.20 0.09 0.03	0.05 -0.11 -0.37	-0.50 -0.63 -0.26	M/M Hull'sCM				
M/M RadCirc	-0.21 -0.17 -0.15	-0.12 -0.01 0.13	0.07 0.03 -0.07	0.53 0.31 0.36	-0.58 -0.31 -0.40	0.36 -0.02 -0.14	-0.06 -0.07 -0.21	-0.63 -0.54 -0.37	0.68* 0.76* 0.71*	M/M RadCirc			
1/2half	-0.09 -0.03 0.13	-0.22 -0.16 -0.24	0.17 0.25 0.29	0.24 0.07 0.29	-0.29 -0.08 -0.33	0.36 -0.27 -0.41	0.11 0.21 0.22	-0.43 -0.30 -0.45	0.19 0.11 0.11	0.17 0.06 0.13	1/2half		
in50/out50	-0.11 -0.25 0.08	-0.17 -0.12 -0.27	0.01 -0.20 0.22	0.13 -0.09 0.12	-0.19 0.06 -0.18	0.29 -0.14 -0.18	-0.04 -0.22 0.19	-0.26 -0.12 -0.33	0.15 0.05 0.17	0.27 0.07 0.31	-0.002 -0.29 -0.06	in50/out50	
Perimeter	0.83* 0.74* 0.66*	-0.56 -0.59 -0.69	0.86* 0.89* 0.78*	0.01 0.02 0.03	0.06 0.008 -0.05	-0.12 -0.47 -0.22	0.90* 0.93* 0.87*	0.09 0.17 -0.22	-0.04 -0.13 -0.42	-0.11 -0.09 -0.30	0.06 0.09 0.05	-0.03 -0.18 0.21	Perimeter
Round out	0.23 0.17 -0.10	0.32 0.13 0.27	-0.19 -0.28 -0.36	-0.82* -0.70* -0.89*	0.92* 0.71* 0.94*	-0.57 0.24 0.45	-0.02 -0.12 -0.23	0.85* 0.71* 0.80*	-0.48 -0.57 -0.43	-0.62 -0.48 -0.46	-0.35 -0.17 -0.38	-0.22 0.02 -0.25	0.03 -0.03 -0.05

Table 1. Correlation matrix of cell morphology descriptors. In each cell r values for animals in order: *A. Japonica*, *C. brevisiphonata*, *P. pectinifera*. * - significant correlation between parameters (among all of the animals); † - significant species-specific correlation (grouping descriptor))

	Mean	Confidence - \+95.000%	Mean	Confidence - \+95.000%	Mean	Confidence - \+95.000%
	A. japonica	*A. japonica*	*C. brevisiphonata*	*C. brevisiphonata*	*P. pectinifera*	*P. pectinifera*
Area	257566	241635-273497	240782	230346-251219	209396*	192867-225926
Circ	0.2181*	0.2097- 0.2266	0.09001*	0.0845- 0.0954	0.1736*	0.1611-0.1861
Round	0.6732*	0.6591-0.6873	0.6457	0.6326-0.6586	0.6402	0.6222-0.6582
Density	0.6054	0.5976-0.6131	0.3888*	0.3781-0.3994	0.6247	0.6073-0.6422
Hull'sPer	2150.97*	2077.2-2224.7	3121.09*	3044.6-3197.5	2449.82*	2308.9-2590.7
Hull'sCirc	0.8534*	0.8463-0.8605	0.8115	0.8056-0.8173	0.8229	0.8148-0.8311
M/M Hull'sCM	1.8111*	1.7776-1.8447	1853608	1.6679-1.7271	1951493	1.6836-1.765
1/2half	1.895	1.7819-2.008	7.0679*	6.2945-7.8411	15008	2.0431-2.3452
in50/out50	0.9951	0.9258-1.0644	1.8114*	1.7106-1.9122	1.0216	0.975-1.0683

Table 2. Average values and their confidence intervals for cell morphology descriptors. * - significant difference between descriptors of different species

A. japonica: C. brevisiphonata			A. japonica: P. pectinifera			C. brevisiphonata: P. pectinifera		
	t-value	p		t-value	p		t-value	p
Area	2087363	0.078400	Area	4.0387	0.000050	Area	471589	0.000930
Circ.	25.4720	0.000000	Circ.	6.0008	0.000000	Circ.	-13.5236	0.000000
Round	2354386	0.004660	Round	2507423	0.004100	Round	0.4928	0.622220
Density	31.6484	0.000000	Density	-2.1856	0.029080	Density	-24.0048	0.000000
Hull'sPer	-17.8892	0.000000	Hull'sPer	-4.0151	0.000060	Hull'sPer	2624482	0.000000
Hull'sCirc	9.0149	0.000000	Hull'sCirc	1157576	0.000000	Hull'sCirc	-2.3069	0.021250
M/MHull'sCM	5.0136	0.000001	M/MHull'sCM	228703	0.001180	M/MHull'sCM	-1.0721	0.283910
1/2half	-12.3948	0.000000	1/2half	-3.1783	0.001520	1/2half	2659941	0.000000
in50/out50	-12.8456	0.000000	внутр50/внеш50	-0.5745	0.565760	in50/out50	2571979	0.000000

Table 3. Results of paired t-test comparison of cell descriptors of all species